

Functionalized vertically aligned ZnO nanorods for application in electrolyte-insulator-semiconductor based pH sensors and label-free immuno-sensors

Narendra Kumar^{1,3}, Sujata Senapati¹, Satyendra Kumar^{2,3}, Jitendra Kumar¹, and Siddhartha Panda^{1,2,3,*}

¹Materials Science Programme, Indian Institute of Technology Kanpur, Kanpur-208016, India

²Department of Chemical Engineering, Indian Institute of Technology Kanpur, Kanpur-208016, India

³Samtel Centre for Display Technologies, Indian Institute of Technology Kanpur, Kanpur-208016, India

*E-mail:- spanda@iitk.ac.in

Abstract. Vertically aligned ZnO nanorods were grown on a SiO₂/Si surface by optimization of the temperature and atmosphere for annealing of the seed. The seed layer annealed at 500 °C in vacuum provided well separated and uniform seeds which also provided the best condition to get densely packed, uniformly distributed, and vertically aligned nanorods. These nanorods grown on the substrates were used to fabricate electrolyte-insulator-semiconductor (EIS) devices for pH sensing. Etching of ZnO at acidic pH prevents the direct use of nanorods for pH sensing. Therefore, the nanorods functionalised with 3-aminopropyltriethoxysilane (APTES) were utilized for pH sensing and showed the pH sensitivity of 50.1 mV/pH. APTES is also known to be used as a linker to immobilize biomolecules (such as antibodies). The EIS device with APTES functionalized nanorods was used for the label free detection of prostate-specific antigen (PSA). Finally, voltage shifts of 23 mV and 35 mV were observed with PSA concentrations of 1 ng/ml and 100 ng/ml, respectively.

1. Introduction

ZnO nanostructures have been extensively studied to develop various potentiometric and field effect based chemical and bio-sensors because of their large surface area to volume ratio and compatibility with biomolecules [1-9]. The chemical functionalization of these nanostructures with 3-aminopropyltriethoxysilane (APTES) prevents etching at acidic pH values [10], and also helps to improve their pH sensing characteristics as obtained in a functionalized ZnO nanowires based liquid gated transistor [11]. The amine groups of the APTES and the polyethylenimine (PEI) are also used as linker molecules to immobilize capture biomolecules (proteins) to develop different immunoassays [12]. Therefore, in addition to their protection at acidic pH values, the improved pH sensitivity of chemically functionalized ZnO nanorods (NRs) could also obviate the need of chemical functionalization and high-k dielectrics such as Si₃N₄, Al₂O₃, and Ta₂O₅ in the fabrication of the enzymatic bio-sensors [13-15]. In order to maximize the surface area to volume ratio of sensing



surface, it is necessary to obtain vertically aligned ZnO nanorods. The microstructure of the seed layer is crucial to obtain the desired orientation and density of the nanorods which could be controlled by the concentration of the ZnO colloid and the annealing temperature of the deposited films [16, 17]. Therefore, it is necessary to obtain a seed layer with well separated and uniform seed particles by varying its annealing temperature and environment. Recently, an electrolyte-insulator-semiconductor (EIS) structure using RF sputtered ZnO thin film was used for pH and multiple ion detections [18]. As per the best of our knowledge, we are not aware of any report on the utilization of functionalized nanorods in the EIS structure for pH and label free detection of prostate-specific antigen (PSA).

In this work, first the effect of temperature and atmosphere on annealing of the ZnO seed layer was studied to obtain the densely packed and vertically aligned nanorods. The properties of grown nanorods were studied with an X-ray diffraction and UV-Vis absorption. Then the as grown and functionalized nanorods grown over SiO₂/Si substrates were studied with field emission scanning electron microscope (FESEM) and X-ray photoelectron spectroscopy (XPS) analysis. The pH sensing characteristics of the EIS devices with the bare and the functionalized nanorods were studied followed by their application for label free detection of PSA.

2. Fabrication and characterization

2.1. Seed layer preparation, growth of nanorods, and chemical functionalization

The 0.75 M zinc acetate dihydrate (ZAD) was dissolved in 40 ml isopropyl alcohol (IPA) followed by stirring the mixture at 60 °C for 45 min at 1000 rpm in a 50 ml glass autoclavable bottles caps, stirred at 1000 rpm for 15 min at room temperature. Subsequently, the complexing agent monoethanolamine (MEA) in equimolar of zinc ions was added at 60 °C and stirred for another 15 min at 1000 rpm till solution became transparent. To get the fine seed solution, the solution was heated in two steps- in a vacuum oven first for 1 hour at 120 °C, and then at 80 °C for 2 hour, and subsequently cooled down to room temperature. The prepared seed solution was spin coated on a piranha cleaned SiO₂/Si substrates at 400 rpm for 1 minute and post baked for 10 minutes at 250 °C on a hot plate. To further improve the seed quality, the films were further annealed at different temperatures in air and vacuum. To grow the nanorods, aqueous solutions of 2 mM zinc nitrate hexahydrate (ZHN) with equimolar hexamine was prepared in 50 ml deionized (DI) water by stirring at 60 °C for 1 hr. The prepared ZnO seed layer over SiO₂/Si substrates were dipped in the prepared solution and the vessel was sealed, followed by heating for 4h at 90°C. After growth of nanorods the samples were thoroughly washed with a stream of DI water to remove the adsorbed nanorods and dried with nitrogen. APTES of purity 99.9% was purchased from Sigma Aldrich, Germany. For the functionalization with APTES, nanorods grown samples were kept in 3% APTES in toluene for 24h and washed with warm toluene, ethanol, and dried with nitrogen.

2.2. EIS device fabrication and characterization

The process steps to fabricate the EIS device were similar to those used in our previous works [19, 20]. The SiO₂/Si wafers of size 1.5 x 1.5 cm² with grown ZnO nanorods were processed using photolithography of SU-8 epoxy for the fabrication of a double step reservoir. The front and back contacts were fabricated by depositing Au (10 mm x 0.3 mm) and Al over the second step of the reservoir and back side of SiO₂ etched silicon, respectively. The Ag/AgCl ink was screen printed over the gold electrode using a mask of 6 mm x 0.5 mm to make the integrated reference electrode. Capacitance-voltage measurement (C-V) measurements were conducted with the help of an impedance analyzer (Model: Agilent 4294A). The sensitivity was measured by normalizing the C-V curves and measuring the reference voltage at 0.5C_{normalized} with buffer solutions of the respective pH values followed by linear fitting of the reference voltages versus the pH values [19]. The EIS device with APTES functionalized nanorods was treated with 10% glutaraldehyde in DI water for 1h, washed with DI water and dried in nitrogen. Then, the antibodies (anti-PSA) were attached by filling the reservoir with 20 µl of anti-PSA solution of concentration 0.1 mg/ml in phosphate buffer saline (PBS)

for 16h at 4 °C and washed thrice with PBS, and dried in nitrogen. The PSA antigens were bound by filling the reservoir of 20 μ l PSA solution of different concentrations range of 1 ng/ml to 1 μ g/ml for 30 minutes at 37 °C. FESEM (Model: JSM-7100F; JEOL) for the imaging of ZnO seed and nanorods. X-ray diffractometer (Model: Panalytical XPert) and spectrophotometer (Model: Varian 5000) were used for phase analysis and band gap measurement, respectively. XPS (PHI 5000 Versa Probe II) was used for the surface analysis of the as grown and functionalized nanorods.

3. Results and discussion

3.1. Effect of seed layer annealing

Growth of vertically aligned ZnO nanorods was realized with a hydrothermal process by optimization of seed layer. The prepared seed layers were annealed at 400 and 500 °C in air as well as in vacuum. As can be seen from figure 1, seed layer annealed in vacuum showed an increase in the average seed size from 16.6 ± 1.4 nm to 25.8 ± 3.8 nm with increase in the annealing temperature from 400 to 500 °C. While no significant changes were observed when annealed in air except flaky structures were observed upon annealing at 500 °C. No growth of nanorods was seen on as prepared seed layer (figure 1b) while few adsorbed microrods grown in solution remained on the surface. Some smaller nanorods were grown on the substrate with seed layers annealed at 400 °C in air as well as vacuum. No growth of nanorods was observed on the seed layer annealed at 500 °C in air because of the flaky nature of the seed structure. The best (vertical) growth of nanorods (figure 1j) was obtained on the seed layer annealed at 500 °C in vacuum. Therefore, one can conclude that the seed layer with well separated particles facilitates to obtain uniform and vertically aligned nanorods.

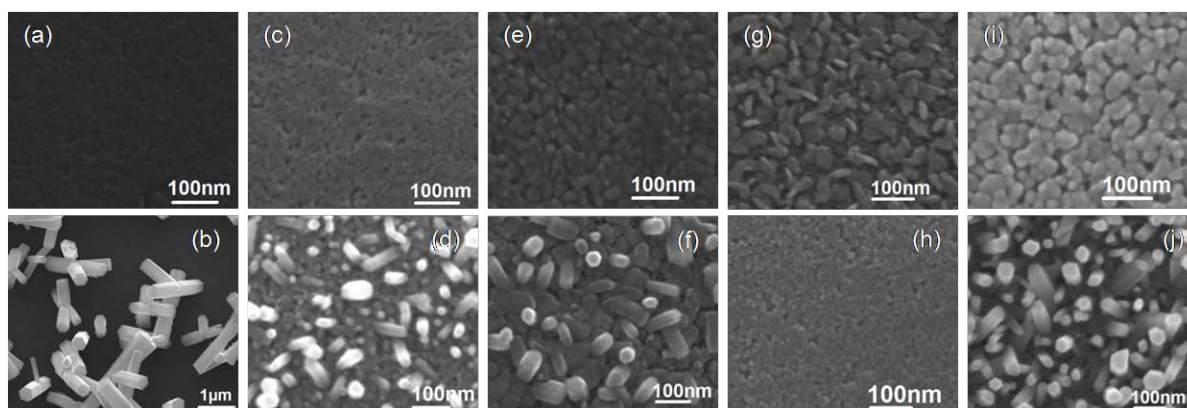


Figure 1. Seed layer as prepared (a) bare (b) with nanorods, Seed layer annealed at 400 °C in air (c) bare (d) with nanorods, Seed layer annealed at 400 °C in vacuum (e) bare (f) with nanorods, Seed layer annealed at 500 °C in air (g) bare (h) with nanorods, Seed layer annealed at 500 °C in vacuum (i) bare (j) with nanorods.

The nanorods grown on the substrate with the seed layer annealed at 500 °C in vacuum were characterized with XRD and UV-Vis absorption and utilized in the fabrication of the EIS device. The XRD pattern shown in figure 2 confirmed the hexagonal wurtzite structure of zinc oxide nanorods with the prominent peaks corresponding to (100), (002), (101), and (103) planes with three smaller peaks corresponding to planes (102), (110), and (112) [21]. The UV-Vis absorption spectra showed the absorption band at wavelength of 383 nm which corresponds to the band gap of 3.24 eV comparable to the reported literature value of 3.21 eV [21].

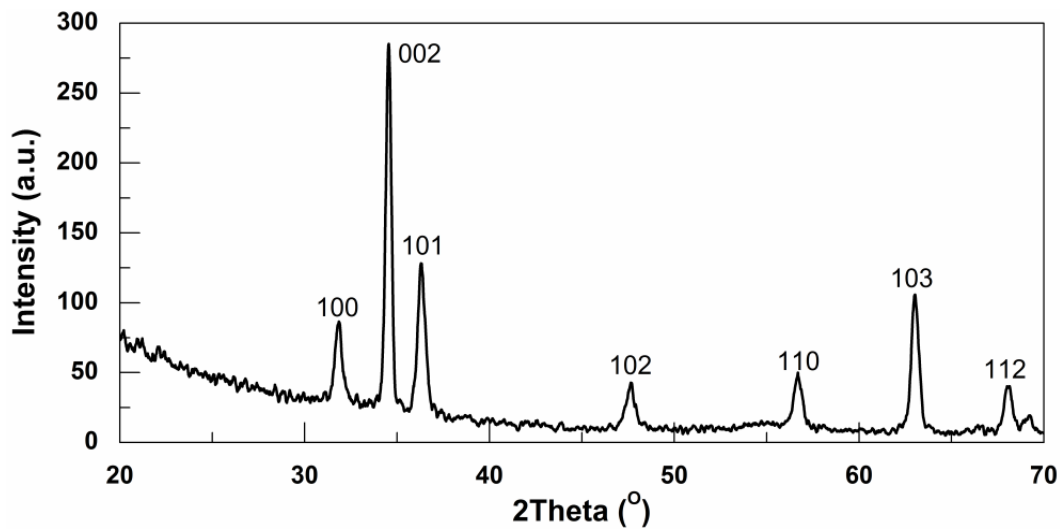


Figure 2. XRD pattern of ZnO NRs grown over SiO_2/Si substrate with the seed layer annealed at 500°C in vacuum. (The peak indices for hexagonal system are in 3-index notation)

3.2. Effect of exposure at acidic pH

The fabricated EIS devices with bare ZnO nanorods were tested for pH detection with pH values decreasing from 9.2 to 4.3. As shown in figure 4, little variation in the capacitance was observed with no significant change in flatband voltage between pH 9.2 to 7.3. Increased capacitance upon exposure of the device with pH 4.3, as seen in figure 3a, could be attributed to the additional layer of ZnO seed and nanorods being etched, and this was supported by the inspection of micrographs, one such being shown in figure 3b, taken after exposing the bare ZnO nanorods based samples with buffer solution of pH 4.3. Also, this was further confirmed as the device showed C-V characteristics and pH sensitivity usually seen for the device only with the SiO_2 dielectric. There are reports available where RF sputtered ZnO films over silicon annealed above 600°C , A-ZnO nanostructures over glass, ZnO nanowires over Cr/Au substrates were utilized for pH sensing [6, 18, 22]. Thus, the etching of ZnO seed and nanorods at acidic pH could be attributed to the poor interface at ZnO/ SiO_2 . In order to overcome this problem, grown nanorods were functionalized with APTES and tested with solution of pH 4.3 and no etching of the surface was observed (micrographs not shown here).

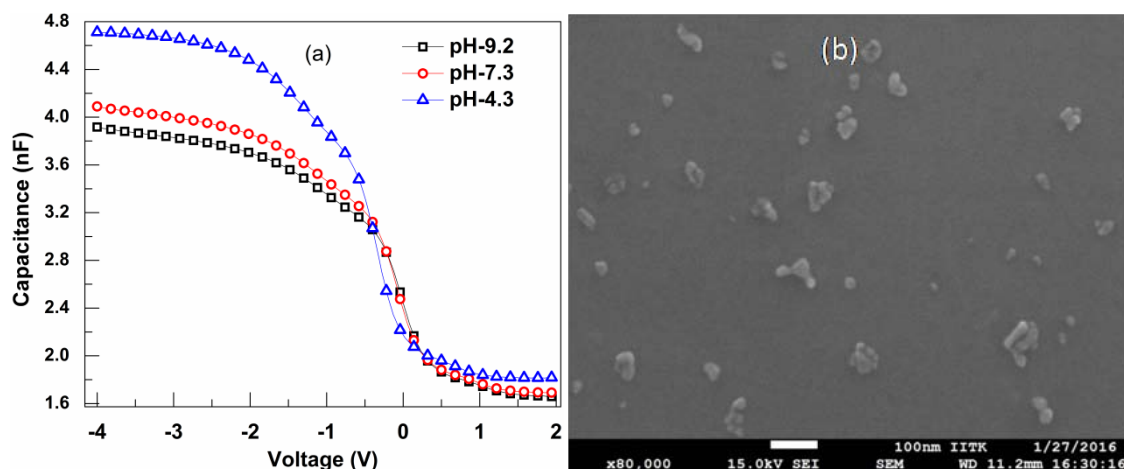


Figure 3. (a) C-V curves of EIS device with bare ZnO nanorods at varying pH values, (b) The micrograph of the sample exposed to pH 4.3.

3.3. Effect of APTES functionalization

The micrographs of ZnO NRs before and after functionalization are shown in figure 4a and 4b, respectively. Figure 4b shows uniformly coated nanorods with APTES resulting in the blunt edges with slightly increased diameter [10]. Figure 5a shows the XPS spectra of bare (as grown) ZnO NRs with three peaks corresponding to C 1s (carbon), O 1s (oxygen), and Zn 2p3 (zinc) at 283.6 eV, 529.4 eV, and 120.3 eV, respectively [23]. Figure 5b shows the XPS spectra with two additional peaks of N 1s (nitrogen) at 397.9 eV and Si 2p (silicon) at 100.8 eV in APTES functionalized nanorods and these are attributed to the amine groups ($-NH_2$) and silane, respectively, in the APTES structure [23-25]. Moreover, the atom weight % of C 1s increased from 16.1 to 29.9 because of ethylene and ethoxy groups in APTES while it significantly decreased from 52.9 to 35.9 for O 1s and from 31.0 to 3.0 for Zn 2p3 upon functionalization due to the coverage of ZnO surface with the APTES molecules.

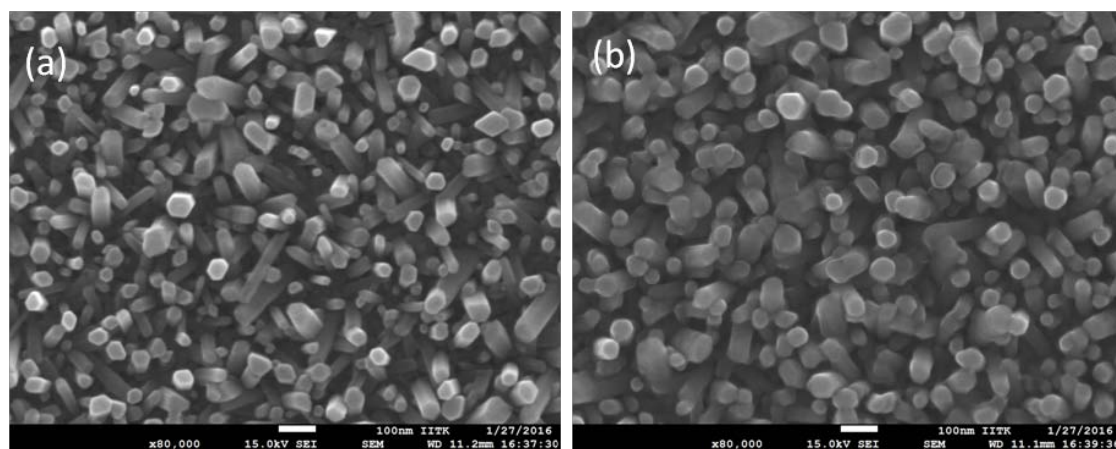


Figure 4. (a) As grown ZnO NRs, (b) APTES functionalized ZnO NRs.

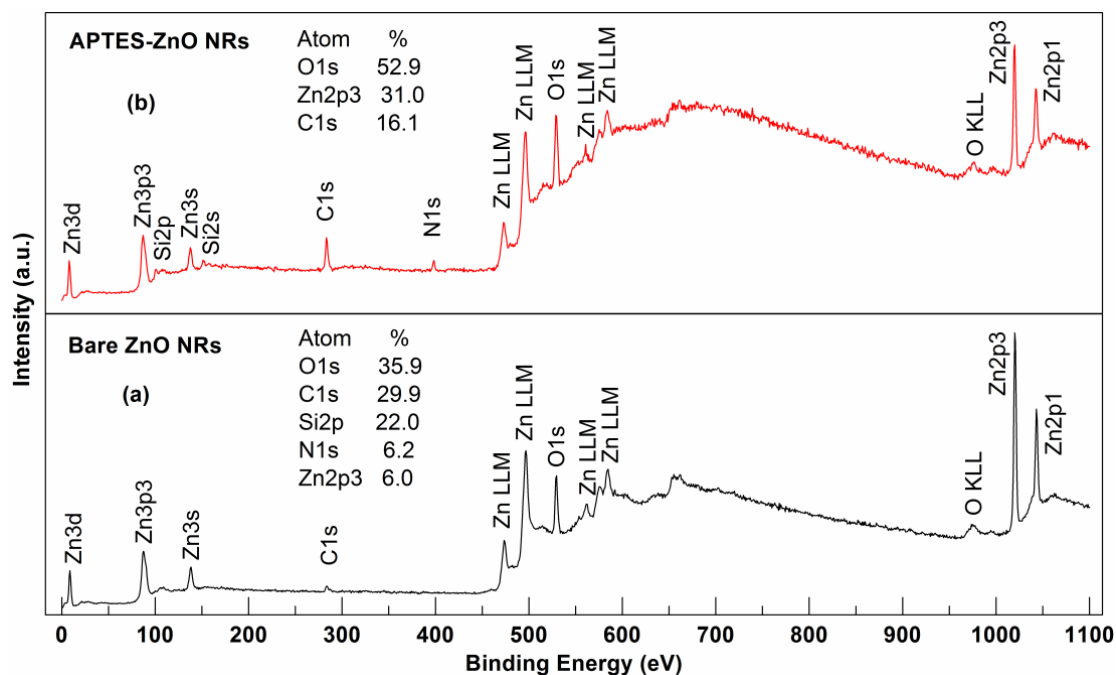


Figure 5. XPS spectra of (a) as grown ZnO NRs (b) APTES functionalized ZnO NRs.

3.4. pH sensing characteristics of functionalized nanorods

Figure 6a shows the C-V curves of the EIS device with APTES functionalized nanorods at varying pH values from 4.3 to 9.2. C-V curves shift towards the positive with increase in pH values because of the increased negative surface charge at the electrolyte/ZnO interface with increasing pH values. Increased negative surface charges induce accumulation in the p-Si without any applied bias resulting in a positive flatband voltage shift. The measured reference voltages at $0.5C_{\text{normalized}}$ with the varying pH values were plotted with respect to pH and the slope obtained by linearly fitting of the plot gives the pH sensitivity. The EIS device with APTES functionalized nanorods showed the average sensitivity of 50.1 mV/pH. The pH sensitivity obtained in this work is higher than the recently reported value (43.2 mV/pH) of APTES functionalized nanowires used in extended gate field effect transistors [22]. Yang et al. [6] obtained a maximum sensitivity of 57.9 mV/pH using Al doped ZnO nanostructures in an extended gate field effect transistor using commercial MOSFETs with high-K dielectrics. However in this work, the SiO_2 was used as dielectric materials to fabricate the EIS device which has a relatively lower dielectric constant (3.9). Therefore, the sensitivity of our devices could further improved by utilizing high-K dielectric materials.

APTES modified ZnO surface contains both type of surface groups $-\text{ZnOH}$ and $-\text{NH}_2$, as confirmed from the XPS spectra of O 1s and N 1s of functionalized nanorods. A similar surface nature ($-\text{OH}$ and $-\text{NH}_2$ groups) has been reported on APTES modified silicon and ZnS/Silica nanowires, which showed a linear pH response [26, 27]. The $-\text{NH}_2$ groups get protonated to $-\text{NH}_3^+$ at acidic pH values while $-\text{ZnOH}$ groups get deprotonated to ZnO at alkaline pH values as reported in our previous work for a SiO_2 surface textured containing $-\text{SiOH}$ and $-\text{NH}_2$ groups with silica nanoparticles via APTES as the linker [28]. Therefore, in addition to the protection of ZnO nanorods from etching at acidic pH values, the APTES modification resulted better the pH sensitivity with a better linearity of 0.99.

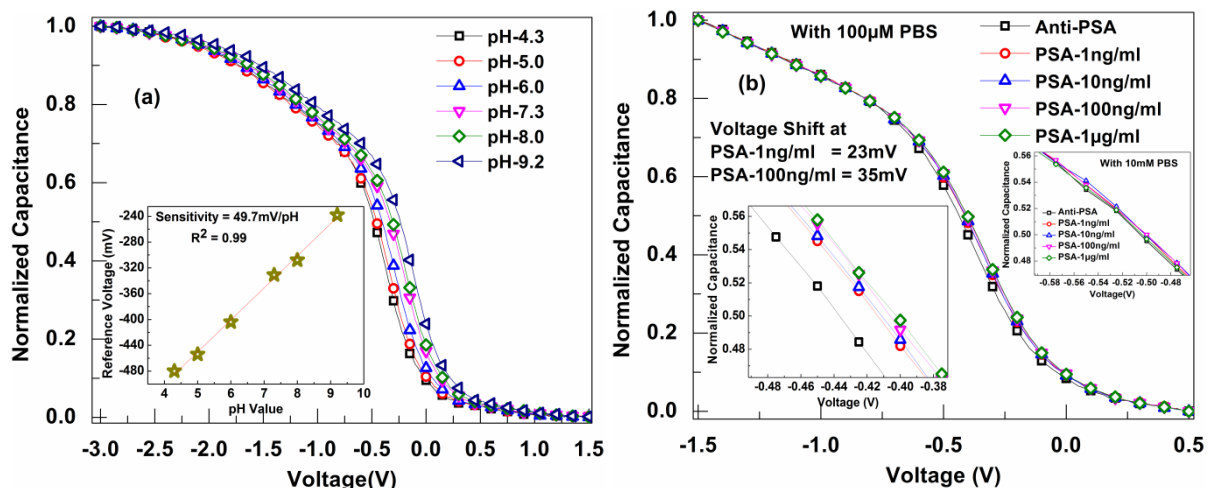


Figure 6. C-V curves of EIS device with APTES functionalized ZnO NRs (a) at varying pH values (the pH sensitivity plot in the inset) (b) at varying PSA concentration measured at 100 μM PBS (for 10mM PBS in the right inset).

3.5. Label-free PSA detection

As discussed in the introduction, in addition to the enhancement of sensitivity of pH detection, the APTES (which acts as a linker) functionalized ZnO nanorods allow the covalent immobilization of biomolecules to utilize them in the development of immuno-sensors. The label-free detection of PSA biomarker has been realized using the EIS device with APTES functionalized nanorods. The PSA biomarker possesses a net negative surface charge at the physiological pH of 7.4. Therefore, the PSA (antigen) binding with immobilized anti-PSA (antibody) on the sensing surface of EIS device induces

the accumulation of holes (majority carriers) in the semiconductor (p-silicon) side. Thus the accumulation of holes without any applied bias results in a positive shift in the flatband voltage. To perform the PSA detection experiment, two strengths of PBS solutions i.e. 10 mM and 100 μ M with 25 mM KCl as ionic strength adjuster [29] were used by taking consideration of the Debye screening effect which remarkably reduces the sensitivity of the device in label-free detection of bioanalytes. As shown in figure 6b (inset right), no significant voltage shift in the C-V curve observed upon binding of PSA of concentration 1ng/ml with 10 mM PBS. While about 23 mV (figure 6b) voltage shift obtained using the PBS solution of 100 μ M at pH 7.4. This notable voltage shift after antigen binding is attributed to the increased Debye screening length with decreased PBS strength [30]. The voltage shift was further increased to a maximum of 35 mV with increased PSA concentration of 100 ng/ml without removing the previously bonded antigens at 1 ng/ml. As shown in figure 6b (left inset), no further voltage shift was observed at higher PSA concentration of 1 μ g/ml, which indicates the maximum numbers of available antibodies immobilized over sensor surface were engaged with antigens of concentration till 100 ng/ml. The calibration curve can be obtained by regenerating the immobilized surface with antibodies by removing the antigen after detection at each concentration and this is the scope of future work.

4. Conclusion

To grow vertically aligned ZnO nanorods with uniform distribution over SiO₂/Si substrates, the seed layer annealing temperature was optimized by annealing in air and vacuum to obtain well separated and uniform seed size. The seeds were not distinguishable in seed layer post baked at 250 °C and formation of nanorods was not observed. Then the samples were annealed at 400 °C and 500 °C for 1h in air as well as in vacuum. The seed layer annealed at 500 °C in vacuum provided well separated and uniform seeds which also proven to be the best condition to get densely packed, uniformly distributed, and vertically aligned nanorods. These SiO₂/Si substrates with nanorods were subsequently utilized to develop an EIS device for pH sensing. The etching of ZnO at an acidic pH 4.3 restricted their direct use for pH sensing. The nanorods were then functionalised with 3-aminopropyltriethoxysilane (APTES) and utilized for pH sensing which showed a pH sensitivity of 50.1 mV/pH. The APTES is also known to be used as linkers to immobilize the biomolecules (antibodies). Thus, the EIS device with APTES functionalized nanorods was used for the label free detection of prostate-specific antigen. Finally, voltage shifts of 23 mV and 35 mV were observed with the PSA concentrations of 1 ng/ml and 100 ng/ml, respectively.

Acknowledgment

The financial support of the DST Science and Engineering Research Board, India (Grant number SB/S3/CE/055/2013) is acknowledged.

References

- [1] Al-Hilli S M, Willander M, Öst A and Strålfors P 2007 *J. Appl. Phys.* **102** 084304
- [2] Ogata K-I, Koike K, Sasa S, Inoue M and Yano M 2009 *J. Vac. Sci. Technol. B* **27** 1684-7
- [3] Kang B S, Wang H T, Ren F, Pearton S J, Morey T E, Dennis D M, Johnson J W, Rajagopal P, Roberts J C, Piner E L and Linthicum K J 2007 *Appl. Phys. Lett.* **91** 252103
- [4] Fulati A, Usman Ali S, Riaz M, Amin G, Nur O and Willander M 2009 *Sensors* **9** 8911
- [5] Usman Ali S M, Nur O, Willander M and Danielsson B 2009 *IEEE Trans. Nanotech.* **8** 678-83
- [6] Yang P-Y, Jyh-Liang W, Chiu P-C, Jung-Chuan C, Cheng-Wei C, Hung-Hsien L and Huang-Chung C 2011 *IEEE Elec. Dev. Lett.*, **32** 1603-5
- [7] Ahmad R, Tripathy N, Jung D-U-J and Hahn Y-B 2014 *Chem. Comm.* **50** 1890-3
- [8] Bhattacharya A, Rao V P, Jain C, Ghose A and Banerjee S 2014 *Mater. Lett.* **117** 128-30
- [9] Ibupoto Z H, Mitrou N, Nikoleli G-P, Nikolelis D P, Willander M and Psaroudakis N 2014 *Electroanalysis* **26** 292-8

- [10] Loh L, Briscoe J and Dunn S 2015 *ACS Appl. Mater. Interfac.* **7** 152-7
- [11] Pachauri V, Vlandas A, Kern K and Balasubramanian K 2010 *Small* **6** 589-94
- [12] Yakovleva J, Davidsson R, Lobanova A, Bengtsson M, Eremin S, Laurell T and Emnéus J 2002 *Anal. Chem.* **74** 2994-3004
- [13] Dzyadevych S V, Soldatkin A P, El'skaya A V, Martelet C and Jaffrezic-Renault N 2006 *Anal. Chim. Act.* **568** 248-58
- [14] Vijayalakshmi A, Tarunashree Y, Baruwati B, Manorama S V, Narayana B L, Johnson R E C and Rao N M 2008 *Biosens. Bioelectron.* **23** 1708-14
- [15] Stepurska K V, Soldatkin O O, Arkhypova V M, Soldatkin A P, Lagarde F, Jaffrezic-Renault N and Dzyadevych S V 2015 *Talanta* **144** 1079-84
- [16] Teng M, Min G, Mei Z, Yanjun Z and Xidong W 2007 *Nanotechnology* **18** 035605
- [17] Tao Y, Fu M, Zhao A, He D and Wang Y 2010 *J. Alloy. Comp.* **489** 99-102
- [18] Haur Kao C, Chen H, Ling Lee M, Chun Liu C, Ueng H-Y, Cheng Chu Y, Jie Chen Y and Ming Chang K 2014 *J. App. Phys.* **115** 184701
- [19] Kumar N, Kumar J and Panda S 2015 *AIP Adv.* **5** 067123
- [20] Kumar N, Tiwari A P, Kumar J and Panda S 2015 *2nd Inter. Symp. Phys. Tech. of Sens. (ISPTS)*, Pune, India: IEEE pp 214-8
- [21] Foo K L, Hashim U, Muhammad K and Voon C H 2014 *Nanos. Res. Lett.* **9** 429
- [22] Qing Z, Wenpeng L, Chongling S, Hao Z, Wei P, Daihua Z and Xuexin D 2015 *Nanotechnology* **26** 355202
- [23] Lee J, Choi S, Bae S J, Yoon S M, Choi J S and Yoon M 2013 *Nanoscale* **5** 10275-82
- [24] Haddada M B, Blanchard J, Casale S, Krafft J-M, Vallée A, Méthivier C and Boujday S 2013 *Gold Bullet.* **46** 335-41
- [25] Zhang W, Luo X-J, Niu L-N, Yang H-Y, Yiu C K Y, Wang T-D, Zhou L-Q, Mao J, Huang C, Pashley D H and Tay F R 2015 *Carriers. Sci. Rep.* **5** 11199
- [26] Cui Y, Wei Q, Park H and Lieber C M 2001 *Science* **293** 1289-92
- [27] He J H, Zhang Y Y, Liu J, Moore D, Bao G and Wang Z L 2007 *The J. Phys. Chem. C* **111** 12152-6
- [28] Kumar N, Kumar J and Panda S 2015 *ECS J. Sol. Stat. Sci. Technol.* **4** N18-N23
- [29] Kumar S, Kumar N and Panda S 2016 *App. Biochem. Biotechnol.* DOI: 10.1007/s12010-016-1986-y
- [30] Jang H-J, Ahn J, Kim M-G, Shin Y-B, Jeun M, Cho W-J and Lee K H 2015 *Biosens. Bioelectron.* **64** 318-23